Computationally Efficient PAPR Reduction schemes in OFDM-Based Satellite Communication Systems

E. Q. Al-Dalakta†, C. C. Tsimenidis†, B. S. Sharif† and A. Al-Dweik†‡
†School of Electrical, Electronic and Computer Engineering, Newcastle University, UK
‡Department of Communication Engineering, Khalifa University, Sharjah, UAE
E-mail:{emad.qeryaqos, charalampos.tsimenidis, bayan.sharif, a.j.al-dweik}@ncl.ac.uk

***Abstract*—Due to the nonlinear characteristics of the high power amplifier (HPA), the employment of orthogonal frequency division multiplexing (OFDM) based modulation schemes results in significant amplitude and phase signal distortion due to the high peak-to-average power ratio (PAPR) nature of the OFDM. To overcome this problem, PAPR reduction methods are commonly applied at the transmitter. Among the plenitude of methods available, partial transmit sequences (PTS) and selected mapping (SLM) are the most powerful schemes. The computational complexity for these schemes is considered as the main disadvantage. In this paper, we propose a low-complexity scheme based on iterative PTS (IPTS) that employs two inverse fast Fourier transforms (IFFT) and two circulant transform matrices. Numerical results demonstrate that the proposed scheme using a partition vector for IPTS with an odd number of ones can achieve both a reduction in PAPR of approximately 2 dB and an improvement of 1.4 dB in terms of signal-to-noise ratio (SNR) to achieve a bit error rate (BER) of 10^{-4}. A further simplification can be achieved by omitting one of the circulant transform matrices in order to improve the computational complexity reduction ratio (CCRR) by 30% and reduce the number of side information bits by 1-bit compared with the IPTS, however, at the cost of a small reduction in PAPR and BER performance.**

***Index Terms*—Orthogonal frequency division multiplexing (OFDM), peak-to-average power ratio (PAPR), high power amplifier (HPA), partial transmit sequence (PTS), selective mapping (SLM), computational complexity reduction ratio (CCRR).**

I. INTRODUCTION

Future satellite communication systems are required to support higher transmission data rates for broadcasting and multimedia services by employing efficient modulation methods such as M-ary quadrature amplitude modulation M-QAM [1]. This type of modulation was introduced for high rate transmission of data such as digital video broadcasting-satellite services to handhelds (DVB-SH). M-QAM is utilized for digital transmission due to its power and spectral efficiency combined with its robustness against nonlinear distortion caused by land mobile satellite (LMS) propagation channels [2].

The employment of single carrier transmission requires high complexity receivers to deal with multipath degradation. To overcome this problem, multicarrier techniques such as orthogonal frequency division multiplexing (OFDM) are employed. However, high peak-to-average power ratio (PAPR) of the transmitted signal is one of the major drawbacks of multicarrier transmission [3].

T. Jiang and Y. Wu, 2008 [4] investigated various techniques exploited in the PAPR reduction such as amplitude clipping, coding, partial transmit sequences (PTS) and selected mapping (SLM). Most PAPR techniques achieve PAPR reduction at the expense of increased transmitted signal power, BER and computational complexity. The PTS and SLM are well known schemes employed for PAPR reduction. These schemes are efficient and distortionless for PAPR reduction however they are more complex than other techniques.

It could be argued that the SLM has at least two advantages compared with the iterative PTS (IPTS). Firstly, the SLM can achieve more PAPR reduction. Secondly, the required bits for side information are less. However, IPTS can be implemented with less complexity. Generally, more complex techniques have better PAPR reduction capability [5].

N. T. Hieu et al, 2005 [6] introduced a low-complexity phase weighting method. In the proposed scheme, only one inverse fast Fourier transforms (IFFT) and one phase weighting matrix were utilized to reduce the system complexity, however, no PAPR reduction was found compared with the PTS technique. C. Wang and Y. Ouyang, 2005 [7] replaced the IFFT blocks applied in the SLM scheme by a kind of low-complexity matrices. Based on the proposed matrices, two novel schemes with low-complexity were proposed. The first method applied only one IFFT, while the second one applied two IFFTs. The simulation showed that the first scheme had worse PAPR reduction performance, while the second had the same reduction as the SLM.

We propose a new low-complexity scheme based on the IPTS (LC-IPTS) that employs two IFFTs and two circulant transform matrices, in order to reduce the complexity and improve the system performance. Furthermore, the low-complexity scheme is simplified (SLC-IPTS) by omitting one of the circulant transform matrices in order to reduce both the computational complexity and the number of side information bits, on the other hand, at the cost of a small reduction in PAPR and BER performance.

This paper is organized as follow: In section II, the system model consisting of the OFDM system and the HPA model are described. Section III explains the construction of the proposed LC-IPTS and SLC-IPTS techniques. Computational complexity for the proposed techniques is formulated in section IV. Computer simulation and results are illustrated in section V, and finally, conclusions are presented in section VI.

978-1-4673-1881-5/12/$31.00 ©2012 IEEE

II. SYSTEM MODEL

A. OFDM system

Let $\mathbf{X} = [X_0, X_1, \ldots, X_{N-1}]_{1\times N}$ represent the input sequence of the IFFT in the frequency domain using N subcarriers. The OFDM signal can be described as [5]-[7],

$$x(t) = \frac{1}{\sqrt{N}} \sum_{n=0}^{N-1} X_n \mathrm{e}^{j2\pi n\Delta f t}, \;\; 0 \leqslant t \leqslant NT, \tag{1}$$

where T is the data period, NT is the OFDM symbol duration and $\Delta f = \frac{1}{NT}$ is the subcarrier spacing. The signal $x(t)$ is sampled to a sequence $\mathbf{x} = [x_0, x_1, \ldots, x_{LN-1}]_{1\times LN}$, where L is the oversampling factor. The oversampled signal can be written as [4] and [6]

$$x_k = \frac{1}{\sqrt{LN}} \sum_{n=0}^{LN-1} X_n \mathrm{e}^{j\frac{2\pi nk}{LN}}, \;\; k = 0, 1, \ldots, LN-1. \tag{2}$$

The main disadvantage of the OFDM signal is the high PAPR, since this signal is a combination of LN modulated subcarriers. The PAPR is defined for a continuous time signal as follows [1] and [3]

$$PAPR = \frac{\max\limits_{0\leqslant t\leqslant NT} |x(t)|^2}{E\{|x(t)|^2\}}, \;\; 0 \leqslant t \leqslant NT, \tag{3}$$

where $E\{|x(t)|^2\}$ represents the average value of power. The theoretical maximum of PAPR for N subcarriers is $10\log_{10}(N)$ dB [3]. The PAPR for the discrete time signal can be estimated by [4]-[6]

$$PAPR = \frac{\max\limits_{0\leqslant k\leqslant LN-1} |\mathbf{x}|^2}{E\{|\mathbf{x}|^2\}}, \;\; k = 0, 1, \ldots, LN-1. \tag{4}$$

It has been proven in [8] that for $L \geqslant 4$, the difference between the continuous-time and discrete-time PAPR is negligible.

B. HPA model

The traveling wave tube amplifier (TWTA) model is commonly utilized in satellite transponders. The amplifier input signal is described by the complex envelope $x(t)$ expressed by [3]

$$x(t) = \rho(t)\mathrm{e}^{j\theta(t)}, \tag{5}$$

where $\rho(t)$ and $\theta(t)$ denote the amplitude and phase of the signal, respectively. The output signal of a HPA can be expressed by

$$y(t) = A[\rho(t)]\mathrm{e}^{j\{\theta(t)+\phi[\rho(t)]\}}, \tag{6}$$

where $A[\rho(t)]$ and $\phi[\rho(t)]$ represent the AM/AM and AM/PM conversion of the nonlinear amplifier, respectively. We have adopted the Saleh TWTA memoryless model, where the AM/AM and AM/PM profiles , respectively, are described as

$$A[\rho(t)] = A_{sat}^2 \frac{\rho(t)}{\rho^2(t) + A_{sat}^2}, \tag{7}$$

$$\phi[\rho(t)] = \frac{\pi}{3} \frac{\rho^2(t)}{\rho^2(t) + A_{sat}^2}. \tag{8}$$

In these equations, A_{sat} represents the amplifier input saturation voltage.

The operating point of the HPA is selected by either the input back-off (IBO) or the output back-off (OBO). The two parameters can be defined as $IBO = 10\log_{10}\frac{P_{in,max}}{P_{av,in}}$ and $OBO = 10\log_{10}\frac{P_{out,max}}{P_{av,out}}$, respectively, where $P_{av,in}$ and $P_{av,out}$ are the average powers of the signal at the input and output of amplifier, respectively, $P_{in,max}$ is the maximum input power (saturation) and $P_{out,max}$ is the maximum output power due to the maximum input power.

III. A NEW SCHEME FOR PAPR REDUCTION

In this section, a new low-complexity (LC-IPTS) technique is proposed for PAPR reduction. In this technique, we employ only two IFFTs and two circulant transform matrices $\mathbf{T}_r$ to reduce complexity and to achieve better performance than the PTS and SLM techniques.

In PTS, the phase factors can be expressed as $\mathbf{b} = [b^{(1)}, b^{(2)}, \ldots, b^{(V)}]_{1\times V}$, while the vector $\hat{\mathbf{b}}$ is the adjacent periodic weighting factors of $\mathbf{b}$ that can be described as $\hat{\mathbf{b}} = [b^{(1)}, b^{(2)}, \ldots, b^{(V)}, b^{(1)}, b^{(2)}, \ldots, b^{(V)}]_{1\times LN}$. If we let $\mathbf{t}_r = \hat{\mathbf{b}}\mathbf{F}^{-1}$, where the transformation $\mathbf{F}^{-1}$ of size $LN \times LN$ is defined as $\mathbf{F}^{-1} = \frac{1}{N} e^{j\frac{2\pi mn}{LN}}$ for $m, n = 0, 1, \ldots, LN-1$, then the circulant transform matrix can be written as [7]

$$\mathbf{T}_r = \begin{bmatrix}\mathbf{t}_r & \mathbf{t}_r^{\langle 1\rangle} & \mathbf{t}_r^{\langle 2\rangle} \cdots \mathbf{t}_r^{\langle LN-1\rangle}\end{bmatrix}^T_{LN\times LN}, \tag{9}$$

where $\mathbf{t}_r^{\langle k\rangle}$ is a circularly right shifted version of the row vector $\mathbf{t}_r$ by element k. The $\mathbf{T}_r$ matrices corresponding to the phase factors $\mathbf{b}$ can be computed off-line and saved in memory.

Fig. 1 shows the new proposed LC-IPTS scheme for PAPR reduction. In this scheme the input data block $\mathbf{X} = [X_0, X_1, ..., X_{N-1}]_{1\times N}$ with N subcarriers is partitioned into two disjoint sets $\mathbf{X}^{(1)} = [X_0, X_1, ..., X_{\frac{N}{2}-1}, 0, ..., 0]_{1\times N}$ and $\mathbf{X}^{(2)} = [0, ..., 0, X_{\frac{N}{2}}, X_{\frac{N}{2}+1}, ..., X_{N-1}]_{1\times N}$. In this figure, we can observe only two IFFTs blocks. The time domain signals $\mathbf{x}^{(l)}$, $l = 1, 2$, are obtained by computing an IFFT of length NL; subsequently, the two disjointed sets are concatenated with $(L-1)N$ zeros. Thus, we can write

$$\mathbf{x}^{(l)} = \mathbf{X}^{(l)}\mathbf{F}^{-1}, \tag{10}$$

where $\mathbf{x}^{(l)} = [x_0^{(l)}, x_1^{(l)}, \ldots, x_{LN-1}^{(l)}]_{1\times LN}$. The time domain signals are multiplied by the circulant transform matrices $\mathbf{T}_r^{(l)}$ and added together to obtain $\mathbf{x}_T$ which can be represented by

$$\mathbf{x}_T = \mathbf{x}^{(1)}\mathbf{T}_r^{(1)} + \mathbf{x}^{(2)}\mathbf{T}_r^{(2)} \;\; = \mathbf{x}_T^{(1)} + \mathbf{x}_T^{(2)}. \tag{11}$$

Fig. 2 shows the proposed SLC-IPTS scheme. The main difference between the LC-IPTS and SLC-IPTS schemes is that the upper branch in the latter scheme does not include $\mathbf{T}_r$. Therefore, the transmitted signal can be simplified to

$$\mathbf{x}_T = \mathbf{x}^{(1)} + \mathbf{x}^{(2)}\mathbf{T}_r \;\; = \mathbf{x}^{(1)} + \mathbf{x}_T^{(2)}. \tag{12}$$

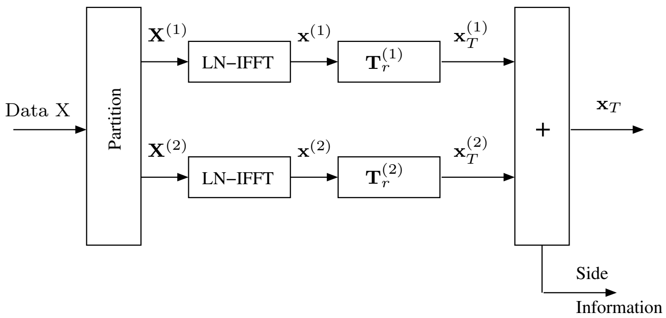

Fig. 1. Block diagram of the proposed LC-IPTS technique.

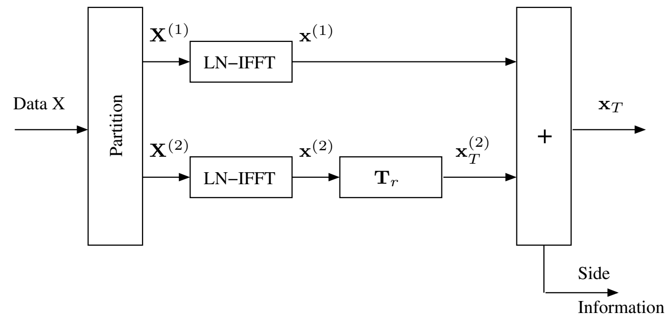

Fig. 2. Block diagram of the proposed SLC-IPTS technique.

Finally, the optimum circulant transform matrices that minimize PAPR are selected for transmission.

In order to recover the information from the transmitted signal, side information is required on which $\mathbf{T}_r$ is employed in the first and second branches. In the receiver, firstly, we perform LN-point fast Fourier transform (FFT) on the received data. The received signal in the absence of noise after the FFT for the LC-IPTS scheme can be given as

$$\mathbf{Y}_b = \left[\mathbf{X}^{(1)}\mathbf{F}^{-1}\mathbf{T}_r^{(1)} + \mathbf{X}^{(2)}\mathbf{F}^{-1}\mathbf{T}_r^{(2)}\right]\mathbf{F}, \tag{13}$$

where the transformation $\mathbf{F}$ of size $LN \times LN$ can be expressed as $\mathbf{F} = e^{-j\frac{2\pi mn}{LN}}$ for $m, n = 0, 1, \ldots, LN-1$. Due to circulant transform matrix properties, the multiplication in (13) can be written as a cyclic convolution [9]

$$\mathbf{Y}_b = \left[\mathbf{X}^{(1)}\mathbf{F}^{-1} \otimes \mathbf{t}_r^{(1)} + \mathbf{X}^{(2)}\mathbf{F}^{-1} \otimes \mathbf{t}_r^{(2)}\right]\mathbf{F}, \tag{14}$$

furthermore, the circular convolution theorem in the Discrete Fourier Transform (DFT) is applied to transform the cyclic convolution into products as shown

$$\mathbf{Y}_b = \mathbf{X}^{(1)}\hat{\mathbf{b}}^{(1)} + \mathbf{X}^{(2)}\hat{\mathbf{b}}^{(2)}, \tag{15}$$

where $\hat{\mathbf{b}}^{(l)} = \mathbf{t}_r^{(l)}\mathbf{F}$, $l = 1, 2$. Similarly, the received signal after the FFT for the SLC-IPTS scheme can be expressed as

$$\begin{aligned}\mathbf{Y}_b &= \left[\mathbf{X}^{(1)}\mathbf{F}^{-1} + \mathbf{X}^{(2)}\mathbf{F}^{-1}\mathbf{T}_r\right]\mathbf{F}, \\ &= \left[\mathbf{X}^{(1)}\mathbf{F}^{-1} + \mathbf{X}^{(2)}\mathbf{F}^{-1} \otimes \mathbf{t}_r\right]\mathbf{F}, \\ &= \mathbf{X}^{(1)} + \mathbf{X}^{(2)}\hat{\mathbf{b}}.\end{aligned} \tag{16}$$

Finally, the signal $\mathbf{Y}_b$ is multiplied by the conjugate matrices of $\hat{\mathbf{b}}$ to recover the transmitted signal.

IV. Computational Complexity

In this section, we will discuss the computational complexity of the LC-IPTS and SLC-IPTS techniques. Generally, the complexity of one LN-point IFFT is $(LN/2)\log_2(LN)$ complex multiplications and $(LN)\log_2(LN)$ complex additions. A complex multiplication, a real multiplication and a complex addition need eighteen, four and two real additions, respectively [10]. The computational complexity equations of the PTS and SLM were derived in [10].

Four cases of phase factors (for $V = 4$ partitions) can be determined (each case has 4 vectors) are shown in Table I. In the odd-case of the circulant transform matrix (number of 1's is odd), $3LN$ complex additions are required. In the even-case, the matrix $\mathbf{T}_r$ has two types, even-case (1) and even-case (2) (number of 1's is even). The first even-case has $2LN$ complex multiplications and LN complex additions. The second even-case has no added computational complexity.

In the LC-IPTS technique, two LN-point IFFTs are required (i.e. $(LN)\log_2(LN)$ complex multiplications and $(2LN)\log_2(LN)$ complex additions). In addition, in the odd-cases, $3ULN$ complex additions are required, where $U = 4$ is the number of circulant transforms performed in each case. In the even-case (1), $2ULN$ complex multiplications and ULN complex additions are needed. Furthermore, the combination of the two sub-blocks requires MLN, where $M = 16$ iteration operations are used for all cases mentioned above. Finally, $2MLN$ real multiplications and MLN real additions are required for power calculation for the cases .

In the SLC-IPTS technique, similar to the first, two LN-point IFFTs are required. As shown in Table I, in the odd-case, $U_1 = 8$ circulant transform matrices are utilized, therefore, we need $3U_1LN$ complex additions. In the even-case, we utilize $U_2 = 8$ circulant transform matrices, therefore, $2(U_2/2)LN$ complex multiplications and $(U_2/2)LN$ complex additions are required. In the full-case, $U = U_1 + U_2$ circulant transform matrices are utilized, $2(U_2/2)LN$ complex multiplications and $3U_1LN + (U_2/2)LN$ complex additions are required. Furthermore, the combination of the two sub-blocks requires U_1LN, U_2LN and ULN for the odd-case, even-case and full-case, respectively. Finally, real multiplications: $2U_1LN$, $2U_2LN$ and $2ULN$ also real additions: U_1LN, $2U_2LN$ and $2ULN$ are required to calculate the power for odd-case, even-case and full-case, respectively.

The overall computational complexity for the PTS, SLM and all proposed cases mentioned above can be formulated in Table II. The computational complexity reduction ratio of the proposed schemes over the PTS or SLM can be defined as [6]

$$CCRR = \left(1 - \frac{x}{y}\right) \times 100\%, \tag{17}$$

where x is the number of real additions for one of the proposed scheme case and y is the number of real additions for the PTS

TABLE I
16 TYPES OF b AND $\mathbf{B}$ FOR V=4 PARTITIONS.

SLC-IPTS	LC-IPTS		$\mathbf{b}$	$\mathbf{B}$ = IFFT $\{\mathbf{b}\}$
full-case	odd-case	odd-case (1)	[1,1,1,-1]	0.5 × [1,j,1,-j]
			[1,1,-1,1]	0.5 × [1,1,-1,1]
			[1,-1,1,1]	0.5 × [1,-j,1,j]
			[-1,1,1,1]	0.5 × [1,-1,-1,-1]
		odd-case (2)	[-1,-1,-1,1]	0.5 × [-1,-j,-1,-j]
			[-1,-1,1,-1]	0.5 × [-1,-1,1,-1]
			[-1,1,-1,-1]	0.5 × [-1,j,-1,j]
			[1,-1,-1,-1]	0.5 × [-1,1,1,1]
	even-case	even case (1)	[1,1,-1,-1]	0.5 × [0,1+j,0,1-j]
			[-1,1,1,-1]	0.5 × [0,-1+j,0,-1-j]
			[1,-1,-1,1]	0.5 × [0,1-j,0,1+j]
			[-1,-1,1,1]	0.5 × [0,-1-j,0,-1+j]
		even-case (2)	[1,-1,1,-1]	0.5 × [0,0,1,0]
			[-1,1,-1,1]	0.5 × [0,0,-1,0]
			[1,1,1,1]	0.5 × [1,0,0,0]
			[-1,-1,-1,-1]	0.5 × [-1,0,0,0]

TABLE II
ANALYSIS OF THE COMPUTATIONAL COMPLEXITY IN THE PTS, SLM AND PROPOSED TECHNIQUES.

PAPR Reduction Technique	Number of equivalent real additions
PTS [10]	$11VLN\log_2(LN) + (2V+7)MLN$
SLM [10]	$11ULN\log_2(LN) + 9ULN$
proposed LC-IPTS odd-case (1) and (2)	$22LN\log_2(LN) + 6ULN + 11MLN$
proposed LC-IPTS even-case (1)	$22LN\log_2(LN) + 38ULN + 11MLN$
proposed LC-IPTS even-case (2)	$22LN\log_2(LN) + 11MLN$
proposed SLC-IPTS odd-case	$22LN\log_2(LN) + 17U_1LN$
proposed SLC-IPTS even-case	$22LN\log_2(LN) + 30U_2LN$
proposed SLC-IPTS full-case	$22LN\log_2(LN) + (11U + 6U_1 + 19U_2)LN$

or SLM scheme. The CCRR can be calculated for the proposed schemes over the IPTS scheme for $N = 128$ subcarriers and $V = U = 4$ partitions. For LC-IPTS, the CCRR is equal to 15% and 21% compared the IPTS with odd-cases and even-case (2), respectively. The even-case (1) is more complex than the IPTS by 12%. For SLC-IPTS, the CCRR is equal to 30% and 7% compared the IPTS with odd-case and even-case, respectively. The IPTS is less complex than the full case by 22%. If the number of subcarriers is fixed, the computational complexity reduction ratio will increase rapidly with increasing partitions since more IFFTs are needed in the SLM or PTS.

V. SIMULATION AND RESULTS

In this paper, we generated 10^5 OFDM blocks randomly with 128 subcarriers ($N = 128$) using 16-QAM data symbols constellation. In addition, the PTS, SLM and proposed techniques are utilized for PAPR reduction. For the IPTS and proposed techniques, the number of allowed phase factors are 2 with random phase values (± 1), while, for the conventional PTS (CPTS) and SLM the number of allowed phase factors are 4 with random phase values ($\pm 1, \pm j$). TWTA with OBO=5 dB and AWGN channel are introduced in our system to assess the BER performance. It is worth noting that the demodulation process is performed based on the assumption of perfect channel knowledge, symbol timing, carrier frequency and phase synchronization.

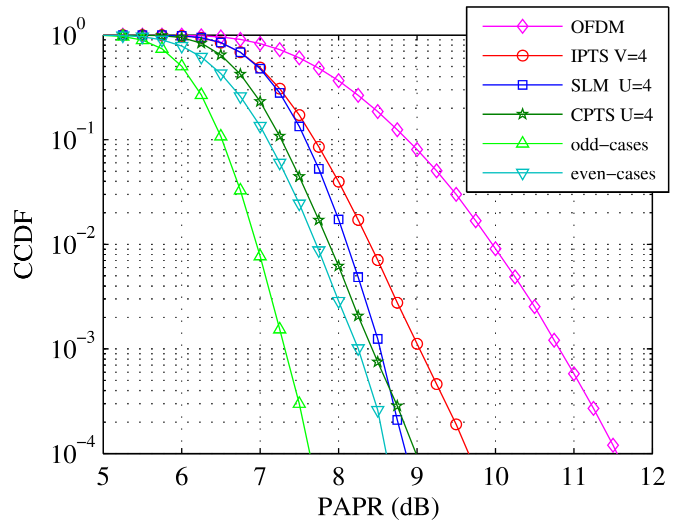

Fig. 3. CCDF of PAPR for the LC-IPTS, IPTS, CPTS and SLM techniques.

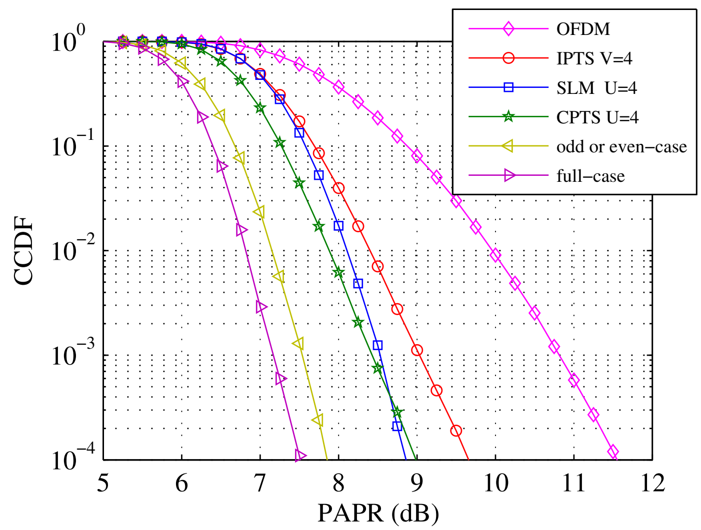

Fig. 4. CCDF of PAPR for the SLC-IPTS, IPTS, CPTS and SLM techniques.

Fig. 3 shows the complementary cumulative distribution function (CCDF) of PAPR for the PTS, SLM and LC-IPTS techniques. It can be seen that the CCDF curve for odd-cases is the best. For example, the odd-cases can achieve 2, 1.4 and 1.2 dB PAPR reduction at 10^{-4} CCDF compared with the IPTS, CPTS and SLM, respectively. Due to the vector $\mathbf{t}_r$ in the odd-cases has a variety of phase weighting factors than in the even-cases; the PAPR reduction of the former is better than the latter. The CCDF curves of PAPR for the PTS, SLM and SLC-IPTS techniques are shown in Fig. 4. From these curves,

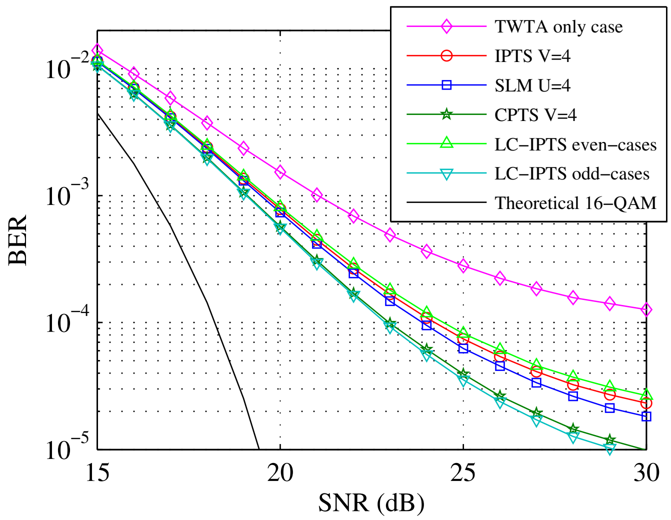

Fig. 5. BER versus SNR for the LC-IPTS, IPTS, CPTS and SLM techniques.

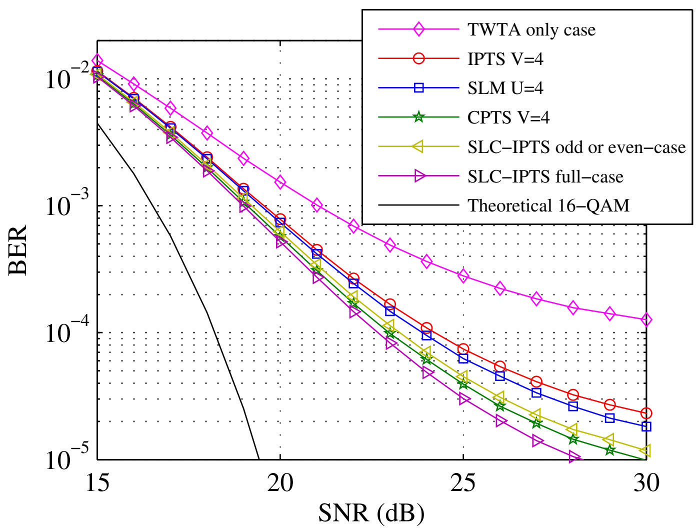

Fig. 6. BER versus SNR for the SLC-IPTS, IPTS, CPTS and SLM techniques.

the PAPR reduction for the full-case is better than odd-case or even-case. In addition, full-case can achieve 2.2, 1.5 and 1.4 dB PAPR reduction, whereas odd-case or even-case can achieve 1.8, 1.1 and 1 dB PAPR reduction compared to the IPTS, CPTS and SLM, respectively. The full-case scheme can achieve better PAPR reduction than the odd or even-case due to the wide range of phase weighting factors of the vector $\mathbf{t}_r$.

Fig. 5 shows the BER performance for various schemes: IPTS, CPTS, SLM and the LC-IPTS. It can be seen that the performance of even-cases is the worst, whilst the BER performance of odd-cases is the best; this is due to the fact that the elements of the phase rotation vector $\mathbf{B}$ for the odd-cases have same amplitude with no zero elements. The odd-cases of the LC-IPTS scheme can achieve an improvement in terms of signal-to-noise ratio (SNR) about 1.4, 1 and 0.1 dB at 10^{-4} BER compared to the IPTS, SLM and CPTS, respectively. Fig. 6 depicts the BER performance for the same schemes mentioned above and the SLC-IPTS. The BER performance in the full-case scheme is the best. The reason of this phenomenon is that the generated vectors of the full-case is double compared with the odd or even-case. This scheme can achieve an improvement 1.6, 1.2 and 0.2 dB, respectively. Whereas, when the odd or even-case is utilized in our system, it can accomplish 1 and 0.6 dB improvement in BER performance compared IPTS and SLM, respectively, and 0.3 dB degradation for CPTS scheme.

VI. CONCLUSION

In this paper, we have proposed a new low-complexity and simplified low-complexity schemes using circulant transform matrices. In these schemes, only two IFFTs are required and the equations of the proposed schemes are derived. The overall computational complexity for the PTS, SLM and proposed schemes are formulated as well. The simulation results show that the proposed LC-IPTS scheme (odd-case) can achieve a reduction in CCRR by 15%. Furthermore, a reduction in PAPR by 2 dB is accomplished. In addition, this scheme can improve BER performance by 1.4 dB. However, the required bits for side information are the same as the PTS scheme. The results of the proposed SLC-IPTS scheme are as follow: 30% reduction in CCRR, 1.8 dB reduction in PAPR, 1 dB improvement in BER performance and the bits requirement for side information are less than the PTS scheme by 1-bit.

REFERENCES

[1] K. Kang, S. Kim, D. Ahn and H.J. Lee, “Efficient PAPR Reduction Scheme for Satellite MC-CDMA Systems,”*IEE Proceedings-Communications,*, vol. 152, no. 5, pp 697-703, Oct. 2005.

[2] ETSI EN 302 583 V1.1.0 , “Digital Video Broadcasting (DVB); Framing Structure, channel coding and modulation for Satellite Services to Handheld devices (SH) below 3 GHz,”2008.

[3] D. Park and H. Song, “A New PAPR Reduction Technique of OFDM System with Nonlinear High Power Amplifier,”*IEEE Trans. Consum. Electron.*, vol. 53, no. 2, pp 327-332, May 2007.

[4] T. Jiang, and Y. Wu, “An Overview: Peak-to-Average Power Ratio Reduction Techniques for OFDM Signals,”*IEEE Trans. Broadcast.*, vol. 54, no. 2, pp 257-268, Jun. 2008.

[5] S. Han, and J. Lee, “An Overview of Peak-to-Average Power Ratio Reduction Techniques for Multicarrier Transmission,”*IEEE Trans. Wireless Commun.*, pp 56-65, Apr. 2005.

[6] N. Hieu, S. Kim and H. Ryu, “PAPR Reduction of the Low Complexity Phase Weighting Method in OFDM Communication System,”*IEEE Trans. on Consum. Electron.*, vol. 51, no. 3, pp 776-782, Aug. 2005.

[7] C. Wang and Y. Ouyang, “Low-Complexity Selected Mapping Schemes for Peak-to-Averag Power Ratio Reduction in OFDM Systems,”*IEEE Trans. Signal Process.*, vol. 53, no. 12, pp 4652-4660, Dec. 2005.

[8] C. Tellambura, “Computation of the Continuous-Time PAR of an OFDM Signal with BPSK Subcarriers,”*IEEE Commun. Lett.*, vol. 5, no. 5, pp 185-187, May 2001.

[9] R. Gray, *Toeplitz and Circulant Matrices: A review,* Foundations and Trends in Communications and Information Theory, vol 2, issue 3, pp 155-239, 2006.

[10] Q. Wen, Y. Xiao, P. Cheng, C. Zhang and S. Li, “S-PTS for PAPR Reduction in OFDM Systems,”*4th Int. Conf. on Wireless Communications, Networking and Mobile Computing*, pp. 1-4, Oct. 2008.